arXiv:hep-ph/9709381v1 17 Sep 1997

# Comprehensive Study of the Possibility of Day - Night Effect Enhancement

Michele Maris
Pavia University - Italy
and
SISSA Trieste - Italy

**Talk held at the:**
*Fourth Solar Neutrino Conference*
April 8 - 11, 1997
Heidelberg, Germany

**Abstract**

A set of quantitative predictions for the D-N asymmetry in the Super - Kamiokande detector is presented. For these predictions, neutrino events are collected in "samples" defined by the trajectories in the Earth of the corresponding solar neutrinos. The more important samples considered here are: the full sample of neutrinos detected at night, the sample of night neutrinos which cross the Earth core and the sample of night neutrinos which does not cross the Earth core. For energy integrated event rates, the D-N asymmetry for core crossing neutrinos is up to six times bigger than the D-N asymmetry for the full sample of night neutrinos. When the reduction in statistics is considered, an effective enhancement up to a factor $\approx 2.3$ is obtained. The selection of core crossing neutrinos may be relevant for the recoil - $e^-$ spectra too. From these results it is reasonable to expect the Super - Kamiokande detector be able to constrain the small mixing angle solution of the solar neutrino problem ($\sin^2 2\theta_v \leq 0.01$) through the D-N effect. Furthermore, it is proposed that the D-N effect may limits the total flux of $^8$B neutrino produced in the Sun. At last, the sensitivity of these predictions to the Earth model uncertainties is quantitatively discussed.

# 1 Introduction

This talk reports the main results from a research conduced by the speaker in collaboration with Serguey T. Petcov (SISSA - Trieste, Italy, also at Institute of Nuclear Research and Nuclear Energy, Bulgarian Academy of Sciences, 1784 Sofia, Bulgaria) and Q.Y. Liu (SISSA - Trieste, Italy) about the Super - Kamiokande sensitivity to the "day-night effect" [1, 2]. The research was aimed by two main purposes: to produce quantitative predictions for the day-night effect as seen by the Super - Kamiokande detector, to study the enhancement in the day-night asymmetry obtained selecting those neutrino events due to solar neutrinos which cross the Earth core in their way to the detector.

The observation of the Earth or day-night (D-N) effect would be a proof of the validity of the MSW solution of the solar neutrino problem, since the Earth effect in neutrino propagation is a direct consequence of neutrino oscillations in matter [3]. In its simplest version the MSW mechanism involves matter - enhanced two-neutrino transitions of the solar $\nu_e$ into an active neutrino $\nu_\mu$ or $\nu_\tau$, $\nu_e \to \nu_{\mu(\tau)}$, while the $\nu_e$ propagates in the Sun. In this case the $\nu_e \to \nu_{\mu(\tau)}$ transition probability depends on two parameters: $\Delta m^2$ and $\sin^2 2\theta_V$, where $\Delta m^2 > 0$ is the neutrino mass squared difference and $\theta_v$ is the angle characterizing the neutrino mixing in vacuum. If $\Delta m^2 \neq 0$ and $\theta_v \neq 0$, the neutrino propagation is sensitive to the matter distribution along the propagation path and the probability to detect at Earth a $\nu_e$ produced in the Sun is a function of the detection time $t$ because at night the Sun is below the horizon and the solar neutrinos cross the Earth reaching the detector, so that further $\nu_e \to \nu_{\mu(\tau)}$ transitions occur. This can lead to a difference or "asymmetry" between the signals caused by the solar neutrinos in a solar neutrino detector during the day and during the night, i.e., to a D-N asymmetry in the signal. No other mechanism of depletion of the solar $\nu_e$ flux proposed so far can produce such an effect.

For the Bahcall and Pinsonneault (1995) solar model and assuming MSW $\nu_e \to \nu_{\mu(\tau)}$ transitions the solar neutrino data can be described for values of the parameters $\Delta m^2$ and $\sin^2 2\theta_V$ belonging to two intervals [6]: $3.6 \times 10^{-6}$ eV$^2 \lesssim \Delta m^2 \lesssim 9.8 \times 10^{-6}$ eV$^2$, $4.5 \times 10^{-3} \lesssim \sin^2 2\theta_V \lesssim 1.3 \times 10^{-2}$; or $5.7 \times 10^{-6}$ eV$^2 \lesssim \Delta m^2 \lesssim 9.5 \times 10^{-5}$ eV$^2$, $0.51 \lesssim \sin^2 2\theta_V \lesssim 0.92$. These intervals correspond to the nonadiabatic (small mixing angle) and to the adiabatic (large mixing angle) solutions of the solar neutrino problem. When theoretical uncertainties in solar neutrino flux components are considered, larger "conservative" regions [5, 6]: $3.0 \times 10^{-6}$ eV$^2 \lesssim \Delta m^2 \lesssim 1.2 \times 10^{-5}$ eV$^2$, $6.6 \times 10^{-4} \lesssim \sin^2 2\theta_V \lesssim 1.5 \times 10^{-2}$; or $7.0 \times 10^{-6}$ eV$^2 \lesssim \Delta m^2 \lesssim 1.6 \times 10^{-4}$ eV$^2$, $0.30 \lesssim \sin^2 2\theta_V \lesssim 0.94$.

To reduce the complexity of the required calculations experimental details such as the background subtraction and the systematic errors were neglected, also continuous data taking, with no interruptions, were assumed. The only experimental constraints which must be considered are: the 5 MeV threshold in the recoil-$e^-$ kinetic energy $T_{e,th}$, and the total yearly event rate for the given threshold energy, which is expected to be $\approx 10^4$ events/year which allows a statistical error $\approx 1\%$ for one year of data. In this way, predictions presented here are for an idealized Super - Kamiokande detector at its best performances. They should be considered the starting point to produce predictions which take in account background, systematic errors and the data taking history. Apart from the Bahcall and Pinsonneault (1995) solar model [4], and the Stacey (1977) Earth model, other source of data are [8].

## 2 Calculating the Earth Effect

The probability for the process $\nu_e \to \nu_e$ for a solar neutrino propagating in the Sun and Earth is given by [9, 10]

$$P_{\oplus}(\nu_e \to \nu_e) = \bar{P}_{\odot}(\nu_e \to \nu_e) + \frac{1 - 2\bar{P}_{\odot}(\nu_e \to \nu_e)}{\cos 2\theta_V}\,(P_{e2} - \sin^2\theta_V), \qquad (1)$$

where $\bar{P}_{\odot}(\nu_e \to \nu_e)$ is the average probability of solar $\nu_e$ survival in the Sun and $P_{e2}$ is the probability of the $\nu_2 \to \nu_e$ transition after the $\nu_e$ have left the Sun. The probability $P_{e2}$ is not a constant in time because it is a function of the trajectory followed by the neutrinos crossing the Earth, determined by the instantaneous apparent position of the Sun in the sky. Given the fact that data are taken over a certain interval of time, the instantaneous $P_{e2}$ in eq. (1) has to be replaced with its time averaged, $< P_{e2} >$, which requires the computation of the solar position in the sky.

For the scopes of D-N effect calculations it is possible to assume for the Earth structure a spherical symmetry, so that the electronic density is radially distributed. In this case the neutrino trajectory and the serie of geological stratifications it crosses reaching the detector are defined by the *Nadir Angle* for the Sun $\hat{h}$, which is the angle between the direction of the Earth center (Nadir) and the direction of the Sun as seen by the detector. From the detection time $t$ of a neutrino event it is possible to recover $\hat{h}(t)$ allowing the selection of events in accord with the trajectory of the incoming neutrinos to form a set of five "samples" labeled: *Day*, *Night*, *Mantle*, *Core* and *Deep - Core*. All the quantities which refers to a specified sample (probabilities, spectra, etc.) are labeled by an index $s = D,\ N,\ C,\ M,\ DC$ for *Day*, *Night*, *Core*, *Mantle*

and *Deep - Core* samples respectively. Samples are defined as follow: the *Day* sample is formed by all neutrino events detected at day; the *Core* sample by those neutrinos which cross the Earth core ($\hat{h} \leq 33.17°$); in the *Mantle* sample neutrinos does not cross the Earth core; ($\hat{h} \geq 33.17°$); the *Night* sample is defined merging the *Core* and *Mantle* sample; at last in the *Deep - Core* sample neutrinos cross the inner 2/3 of core.

The computation of $\bar{P}_{\odot}(\nu_e \rightarrow \nu_e)$ is accomplished following the prescriptions derived in ref. [11].For a given Earth model and a fixed set of values for the parameters $\hat{h}$, $\sin^2 2\theta_V$ and $E_\nu/\Delta m^2$, $P_{e2}$ is computed solving numerically the ordinary differential equations for the neutrino propagation in the Earth. The differential equation is integrated through a $4^{th}$ order Runge - Kutta algorithm with an adaptive step size. A set of tests assures this procedure is stable and accurate at the $\approx 10^{-5}$ level. Furthermore, all over the program checks were made to assure consistency and proper numerical error control, based on the comparison of results obtained by the `FORTRAN` code with results obtained by a `MATHEMATICA` code. The comparison shows relative differences $\approx 10^{-5}$ in all the relevant cases. In conclusion the numerical error is under control and quite negligible.

Apart from the *Day* sample, each sample $s = D,\ N,\ C,\ DC$ requires a different calculation of the time average probability $< P_{e2} >^s$ from the instantaneous probability $P_{e2}$. For a sample $s = D,\ N,\ C,\ DC$ defined by the nadir angle interval $[\hat{h}_1^s, \hat{h}_2^s]$, and obtained over an exposure time interval $[T_1^s, T_2^s]$ (assumed here to last from January $1^{st}$ 1996 to January $1^{st}$ 1997) the averaged $P_{e2}$ probability is defined as:

$$< P_{e2} >^s = \frac{1}{T^s_{res}} \int_{T_1^s}^{T_2^s} dt\, \frac{\hat{\delta}(\hat{h}_1^s \leq \hat{h}(t) \leq \hat{h}_2^s)}{R^2(t)}\, P_{e2}(\hat{h}(t)), \tag{2}$$

where: $\hat{\delta}$ is 0 for $\hat{h}$ outside the nadir angle interval and 1 for $\hat{h}$ inside it; $R(t)$ is the Sun - Earth distance expressed in units of the mean distance (the Astronomical Unit $R_0 = 1.4966 \times 10^8$ km); and

$$T^s_{res} = \int_{T_1^s}^{T_2^s} dt\, \frac{\hat{\delta}(\hat{h}_1^s \leq \hat{h}(t) \leq \hat{h}_2^s)}{R^2(t)} \tag{3}$$

is the *residence time*, i.e., the time spent by the Sun in $[\hat{h}_1^s, \hat{h}_2^s]$. In the absence of neutrino oscillations the total fraction of solar neutrinos induced events in $[\hat{h}_1^s, \hat{h}_2^s]$ is $T^s_{res}/T_y$, where $T_y = (T_2^s - T_1^s)$ in this case is the year length. For the Super - Kamiokande detector the times over one year of data taking are: $T^N_{res}/T_y = T^D_{res}/T_y = 0.5$, $T^C_{res}/T_y = 0.071$, $T^M_{res}/T_y = 0.429$, $T^{DC}_{res}/T_y = 0.0394$.

With a statistics of $10^4$ events this corresponds to a relative statistical error of about 1.4% (*Night* or *Day*), 3.8% (*Core*), 1.5% (*Mantle*), 5.0% (*Deep - Core*). The residence time is also relevant because it weights the contributions to $< P_{e2} >^N$ from each geophysical structure and from the error source.

Many types of systematic errors can affect the predictions for the D-N asymmetry. Since the initial hypothesis, the most relevant error sources for these calculations are related to the Earth model and the apparent solar motion [1].

Earth model uncertainties introduce a relevant error source (especially for the core) since they affects the Earth electronic density $n_e \propto Y_e \rho$, where $Y_e$ is the fraction of electrons per nucleon and $\rho$ is the matter density (in $\mathrm{Dr/cm^3}$), the combined $n_e$ uncertainty is $\approx 7\% \div 10\%$ [2]. Its effect was studied repeating the calculations taking the $\rho$ distribution [7] but for two different hypothesis about $Y_e$ in the core: $Y_e = 0.467$ which is representative of current knowledge and $Y_e = 0.5$ which combines all the uncertainties in Earth models. In both the cases it is assumed $Y_e = 0.5$ in the mantle [1, 2].

The apparent solar motion is quite complex and approximations are required to save computing time. The limit in the accuracy for the Sun's tracking is fixed by the angular diameter of the $^8$B neutrino production region $\approx 3$ arcmin [1]. There are two kinds of approximation made which are relevant for the Earth effect. In the first the Earth motion around the Sun is circular (COA), in the second it is elliptical (EOA), both of them are not exact models, but EOA is very accurate for Earth effect prediction purposes.

The systematic errors in the Sun position produced by the COA and the EOA affect (2) and (3) in two ways: i) they change the time in which the Sun cross the boundaries of a given Nadir angle interval, ii) they change $\hat{h}$(t). The first way is the less relevant, since it mainly affects the residence time, which is the difference between two next crossing times, so that errors compensate. The second way is more relevant, because it affects the length of the neutrino path in a given geological structure. The analysis shows that EOA introduces errors in the Sun position smaller than $0.01^\circ$, while COA may introduce errors as large as few $0.01^\circ$. Most of these errors are periodic in nature, and they should average out. However, since $P_{e2}$ is a function of the solar position and the use of different sampling schemes (as *Core*, *Mantle*, *Night*, etc.) are equivalent to averaging over specific fractions of year only, it is not possible to test such approximations without numerical experiments, the most relevant case being the interplay between the change in flux due to the time dependence in the Sun - Earth distance $R(t)$ and the time dependence in the Earth orbital velocity [1]. In conclusion, all the results presented here are obtained using the EOA, which assures an accuracy for $< P_{e2} >$ largely better than 1% for each kind of sample

and in what regards the solar motion.

## 3 Results

At the basis of each time averaged probability $< P_{e2} >$ is the instantaneous one, $P_{e2}$. Figure 1 shows an example of the probability $P_{e2}$ for $\sin^2 2\theta_V = 0.01$ as a function of $\hat{h}$ and of the *Resonance Density* in the Earth $\rho_R$ (gr/cm$^3$) [1]: $\rho_R Y_e = 6.57 \times 10^6 (\Delta m^2(\ \mathrm{eV}^2)/E_\nu(\ \mathrm{MeV}))\cos 2\theta_V$. There are two main peaks associated to resonance transitions in the core, `C`, and in the mantle `M` [1]. In addition, the spherical symmetry of the Earth implies that solar neutrinos will cross the resonance region twice. Since the neutrino oscillation length in matter, for solar neutrinos which undergo resonance transitions in the Earth, is of the order of the Earth radius, interference terms in $P_{e2}$ lead to oscillatory dependence of $P_{e2}$ on $\hat{h}$ for a fixed $\rho_R$ [1, 10].

Increasing $\sin^2 2\theta_V$, for $\sin^2 2\theta_V < 0.1$, the qualitative properties of this dependences do not change significantly. The two peaks scales accordingly to $\sin^2 2\theta_V$, with `C` increasing faster than `M` reaching a maximum value and begins to decrease while `M` is still increasing. As a consequence, at values of $\sin^2 2\theta_V \lesssim 0.13$ most of the D-N asymmetry is generated by the MSW effect in the core. At larger $\sin^2 2\theta_V$ values the behaviour is more complicate, new peaks appears and (for $\sin^2 2\theta_V \geq 0.3$) the bulk of the Earth transition is in the mantle.

As Fig. 2a illustrates, the separation in *Core* and *Mantle* samples is very effective in enhancing $< P_{e2} >$. The enhancement is particularly large for small mixing angles for which $< P_{e2} >^C$ can be up to six times bigger than $< P_{e2} >^M$ (for $\sin^2 2\theta_V \geq 0.3$ the core - enhancemente is only $30\% \div 40\%$). This suggests the possibility of a corresponding enhancement of the $e^-$-spectrum distortions as well as of the energy integrated event rate. To have an enhancement in the averaged probability $< P_{e2} >$ is not enough to ensure an enhancement in the D-N asymmetry, especially at small mixing angles. The upper "window" of Fig. 2b is a combined plot of $\bar{P}_\odot$ (dotted line), $P_{e2}$ (dashed line) and $P_\oplus$ (solid line) for *Core*. In the lower "windows" there is a plot of the ratio:

$$\mathcal{A}_P^s(E_\nu/\Delta m^2) \equiv 2\ \frac{P_\oplus(E_\nu/\Delta m^2) - \bar{P}_\odot(E_\nu/\Delta m^2)}{P_\oplus(E_\nu/\Delta m^2) + \bar{P}_\odot(E_\nu/\Delta m^2)} \tag{4}$$

which is the D-N asymmetry for the total survival probability. The large peak on the left side of the figure is an artifact of the presence of the adiabatic minimum in the probability $\bar{P}_\odot$. The bulk of the D-N asymmetry comes from the second peak in the figure.

Figure 2 is an example of how each probability contributes in $P_{\oplus}$ and in the related asymmetry. One of the important features that has to be taken into account in the discussion of $P_{\oplus}$ is the position of the peaks in $< P_{e2} >$ with respect to the value of $E_\nu/\Delta m^2$ at which $\bar{P}_{\odot} = 0.5$ because it controls the sign and the magnitude of the D-N effect. It follows from eq. (1) that the asymmetry is zero each time $\bar{P}_{\odot} = 0.5$ irrespective of the value of $< P_{e2} >$. If $< P_{e2} > > \sin^2\theta_V$, and $\bar{P}_{\odot} < 0.5$ ($\bar{P}_{\odot} > 0.5$), the asymmetry is positive (negative) which means the Earth effect *increases* (*reduces*) the night event rate [1]. The presence of a zero Earth effect can reduce the magnitude of the D-N asymmetry. The negative D-N effect is relevant for $\sin^2 2\theta_V < 0.004 \div 0.006$.

The definitions for the recoil-$e^-$ spectrum with (without) MSW effect $\mathcal{S}^s(T_e)$ ($\mathcal{S}_0(T_e)$), $T_e$ being the recoil-$e^-$kinetic energy and $s = D,\ N,\ C,\ M$; and for the energy integrated event rates with (without) MSW effect $\mathcal{R}^s(T_{e,th})$ ($\mathcal{R}_0(T_{e,th})$), $T_{e,th}$ being the recoil-$e^-$threshold kinetic energy, in terms of the survival probability $P_{\oplus}$, are reported in [2] Here it is enough to recall the definition of the distortion for the recoil-$e^-$spectrum due to the MSW effect: $\delta\mathcal{S}^s(T_e) = \mathcal{S}^s(T_e)/\mathcal{S}_0(T_e)$, $s = D,\ N,\ C,\ M$, and the definitions for the D-N asymmetries for the recoil-$e^-$spectrum $\mathcal{A}^s_{D-N}(T_e)$ and the energy integrated event rate $A^s_{D-N}(T_{e,th})$:

$$\mathcal{A}^s_{D-N}(T_e) = 2\,\frac{\mathcal{S}^s(T_e) - \mathcal{S}^D(T_e)}{\mathcal{S}^s(T_e) + \mathcal{S}^D(T_e)}, \qquad A^s_{D-N}(T_{e,th}) = 2\,\frac{\mathcal{R}^s - \mathcal{R}^D}{\mathcal{R}^s + \mathcal{R}^D}, \tag{5}$$

with $s = D,\ N,\ C,\ M$. Both these observable quantities are solar model independent, and are related to $\mathcal{A}^s_P(E_\nu/\Delta m^2)$, $s = D,\ N,\ C,\ M,\ DC$. For fixed values of $\sin^2 2\theta_V$ and $T_{e,th}$:

$$\begin{aligned} \max(A^s_{D-N}) \quad &\approx \quad \frac{\max(\mathcal{A}^s_P(E/\Delta m^2)\bar{P}_{\odot,max}}{\alpha - \beta\ \max(\mathcal{A}^s_P(E/\Delta m^2) + \bar{P}_{\odot,max}}, \\ \mathcal{A}^s_{D-N}(E - 0.5\ \mathrm{MeV}) \quad &\approx \quad \frac{\mathcal{A}^s_P(E/\Delta m^2)\bar{P}_{\odot}(E/\Delta m^2)}{\alpha - \beta\ \mathcal{A}^s_P(E/\Delta m^2) + \bar{P}_{\odot}(E/\Delta m^2)}, \end{aligned} \tag{6}$$

where $s = D,\ N,\ C,\ M,\ DC$, $\alpha = 0.190476$, $\beta = 0.0952381$. In the upper formula $A^s_{D-N}$ is regarded as a function of $\Delta m^2$, $\bar{P}_{\odot,max}$ is the value of $\bar{P}_{\odot}(E_\nu/\Delta m^2)$ computed for the $E_\nu/\Delta m^2$ value which corresponds to the $\mathcal{A}^s_P(E_\nu/\Delta m^2)$ maximum $\max(\mathcal{A}^s_P)$. In the lower formula $\Delta m^2$ is fixed, while it is assumed: $E \cong E_\nu \cong T_e + 0.5$ MeV. Equations (6) overestimate the numerical results by a factor between 3% and 40%. The error decreases increasing $\sin^2 2\theta_V$.

One example of the predicted recoil - $e^-$ spectrum distortion in the Sun, and one example of D-N asymmetries in the spectrum are shown in Figs. 3

(see [2, 13] for a larger set of examples) both the figures being computed for $Y_e = 0.467$. The enhancement of the spectrum distortions and of the D-N asymmetry in the *Core* sample is clearly seen, especially for $\sin^2 2\theta_V \lesssim 0.013$. The differences between the spectra computed for $Y_e = 0.467$ and for $Y_e = 0.5$, are largely negligible for the expected experimental accuracy.

The differences between the *Day* and the *Night* (*Mantle*) sample $e^-$ - spectra are hardly observable, but for $\sin^2 2\theta_V \geq 0.008$ and many values of $\Delta m^2$ from the "conservative" MSW solution region, $\mathcal{A}^C_{D-N}(T_e)$ may reach a value of 10% and even larger ($20\% - 30\%$). So, its measurement can further constrain $\Delta m^2$ and $\sin^2 2\theta_V$ values.

Figures 4, 5 represent the iso-(D-N) asymmetry contour plots for the *Night*, *Core* and *Mantle* samples. Shown are also the "conservative" regions of the two MSW solutions of the solar neutrino problem (dashed lines) as well as the solution regions obtained in the reference solar model [4] (inner thick dashed lines). Also the iso-(D-N) asymmetry contours for the *Night* and *Core* samples shown in Figs. 4 and 5 have been obtained both for $Y_e = 0.467$ (solid lines) and for $Y_e = 0.5$ (dash-dotted lines). For given $\Delta m^2$ and $\sin^2 2\theta_V$ the differences between $A^N_{D-N}$ or $A^M_{D-N}$ and $A^C_{D-N}$ are larger in the NA region. The magnitude of the D-N asymmetry in the AD region does not change significantly with the change of the sample. In contrast, in the NA region the D-N asymmetry in the *Core* sample is enhanced by a factor of up to six. The reduction in statistics for this sample reduces it to an effective 2.3 enhancement. From Fig. 5 it comes that the *Core* selection is a very effective method to enhance the D-N asymmetry despite the loss of statistics.

The difference between the values of the *Core* sample asymmetry $A^C_{D-N}$ calculated for $Y_e = 0.467$ and for $Y_e = 0.5$ depends strongly on the values of $\Delta m^2$ and $\sin^2 2\theta_V$. However, Figs. 5 show that the main results illustrated here are stable against the Earth model uncertainty [2].

Because of the large differences between the core and the mantle structures, the *Mantle* and *Core* subsamples provide two independent measurements of the D-N effect. These can be combined to constrain better the neutrino parameters $\Delta m^2$ and $\sin^2 2\theta_V$, utilizing the full statistics of the *Night* sample, especially in NA region [2].

Figs. 5 suggests also the possibility to use the D-N effect to limit the $^8$B neutrinos total flux [2].

## 4 Conclusions

In this talk the possibility of a core-enhancement for the D-N effect in the Super - Kamiokande detector, proposed by example in [10], was discussed in detail. It was remarked the need of a precise apparent solar motion reconstruction to produce the accurate D-N effect predictions required to study this subject. A computer code which fulfills this requirement was presented. Predictions for Super - Kamiokande detector observable quantities were obtained. It was shown that: I). The *Core* sample D-N asymmetry can be enhanced up to factor six compared to the *Night* and *Mantle* D-N asymmetries. The enhancement reduces to a factor 2.3 when the loss in statistics is properly accounted for. If Super - Kamiokande will be able to reach an accuracy of some percent in measuring the *Core* D-N asymmetry it is reasonable to expect it will be able to test this region through the D-N effect. II). The enhancement may be relevant for the recoil-$e^-$ spectra distortion and the recoil-$e^-$ spectra D-N asymmetry. III). The detection (or lack of detection) of a small D-N asymmetry may constraint the total $^8$B neutrino flux from the Sun in a solar model independent way (presently this flux is uncertain for a factor two). IV). These results are qualitatively robust against the Earth model uncertainties.

## Acknowledgments

The author is deeply indebted with Prof. W. Hampel and the organizing committee of the *Fourth International Solar Neutrino Conference* for the kind concession of a financial support to attend to the conference. This research was partially supported by S.I.S.S.A. Trieste, Italy, research contracts: 4060 and 5566.

## References

[1] Q.Y. Liu, M. Maris and S.T. Petcov, Preprint SISSA 16/97/EP, January 1997, E-archive report hep-ph/9702361.

[2] M. Maris and S.T. Petcov, SISSA Report ref. SISSA 17/97/EP, May 1997, E-archive report hep-ph/9705392.

[3] S.P. Mikheyev and A.Yu. Smirnov, Sov. J. Nucl. Phys. **6**, 913 (1985); L. Wolfenstein, Phy. Rev. D **20**, 2369 (1978).

[4] J.N. Bahcall and M.H. Pinsonneault, Rev. Mod. Phys. **67**, 781 (1995).

[5] P.I. Krastev and A.Yu. Smirnov, Phys. Lett. B **338**, 282 (1994); V. Berezinsky. G. Fiorentini and M. Lissia, *ibid.* B**341**, 38 (1994); N. Hata and P. Langacker, Phys. Rev. D**52**, 420 (1995).

[6] P.I. Krastev and S.T. Petcov, reported by S.T. Petcov at the "Neutrino'96" International Conference on Neutrino Physics and Astrophysics, June 13-19, 1996, Helsinki, Finland.

[7] F.D. Stacey, *Physics of the Earth, $2^{nd}$ edition*, John Wiley and Sons, London, New York, 1977.

[8] J.N. Bahcall et al., Phys. Rev. D **54**, 411 (1996). J.N. Bahcall, M. Kamionkowski and A. Sirlin, Phys. Rev. D **51**, 6146 (1995).

[9] S.P. Mikheyev and A.Yu. Smirnov, in *Massive Neutrinos in Astrophysics and in Particle Physics*, Proceedings of the Moriond Workshop, Tignes, Savoie, France, 1986, edited by O. Fackler and J. Tran Thanh Van (Editions Frontières, Gif-sur-Yvette, France, 1986), p. 355; in *New and Exotic Phenomena*, Les Arc, Savoie, France, 1987, edited by O. Fackler and J. Tran Thanh Van (Editions Frontières, Gif-sur-Yvette, France, 1987), p. 405.

[10] A.J. Baltz and J. Weneser, Phys. Rev. D **50**, 5971 (1994).

[11] S.T. Petcov, Phys. Lett. B **200**, 373 (1988). P.I. Krastev and S.T. Petcov, Phys. Lett. B **205**, 84 (1988).

[12] B. Bertotti and M. Maris, *Variabilitá Temporale del Flusso di Neutrini Solari in Esperimenti Sotterranei* (*Neutrino Flux Time Variability in Underground Experiments*), reported in the Ph. D. thesis of M. Maris, Department of Theoretical and Nuclear Physics (D.F.N.T.), Pavia University, 1996, Italy.

[13] M. Maris and S.T. Petcov, E-archive report hep-ph/9703207, February 1997.

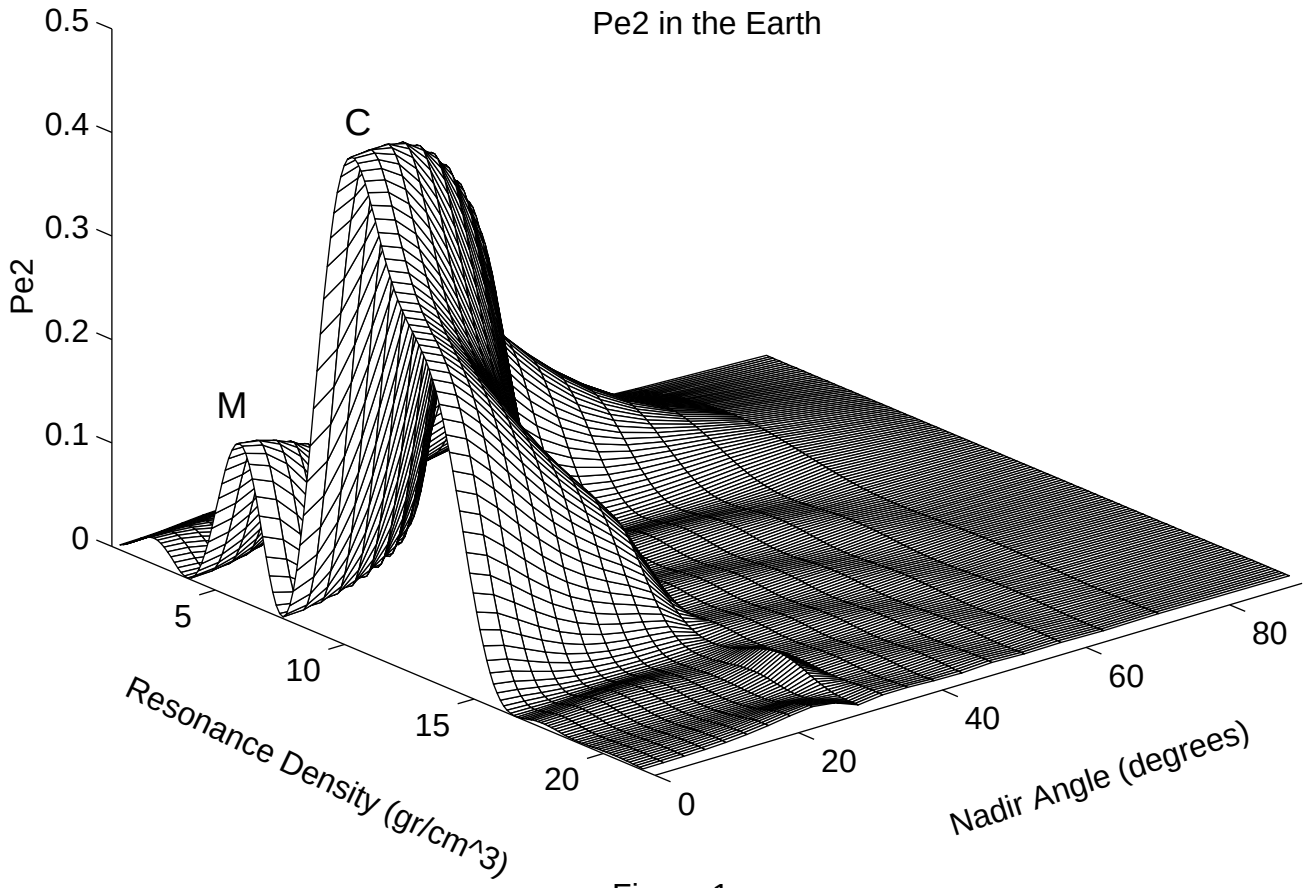
Pe2 in the Earth
Pe2
0.5
0.4
0.3
0.2
0.1
0
C
M
5
10
15
20
Resonance Density (gr/cm^3)
0
20
40
60
80
Nadir Angle (degrees)

Figure 1

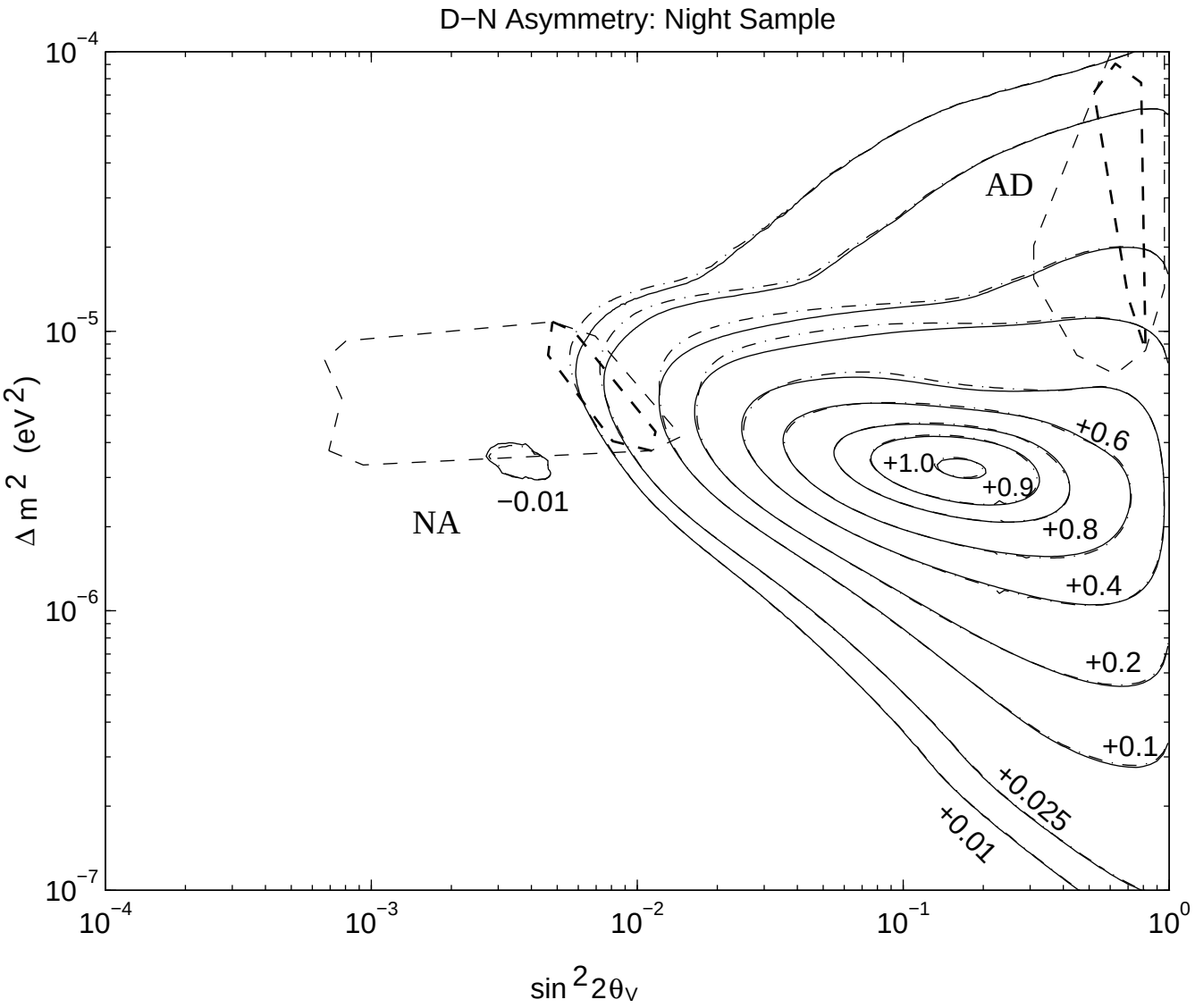
D−N Asymmetry: Night Sample
AD
NA
−0.01
+1.0
+0.9
+0.8
+0.6
+0.4
+0.2
+0.1
+0.025
+0.01
$10^{-4}$
$10^{-5}$
$10^{-6}$
$10^{-7}$
$10^{-4}$
$10^{-3}$
$10^{-2}$
$10^{-1}$
$10^{0}$
$\Delta m^2$ (eV$^2$)
$\sin^2 2\theta_V$

Figure 4

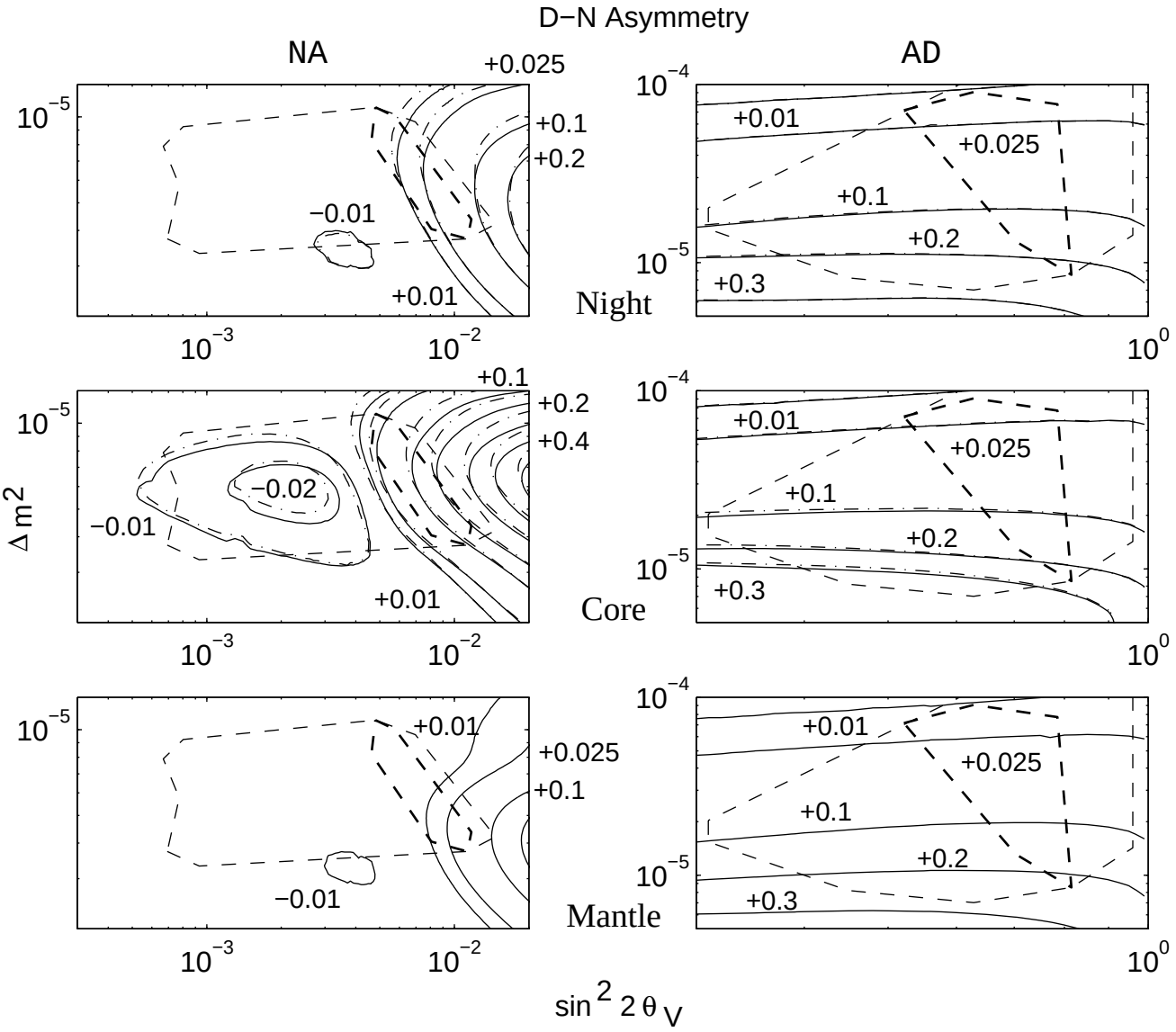
D−N Asymmetry
NA
AD
+0.025
+0.1
+0.2
−0.01
+0.01
+0.01
+0.025
+0.1
+0.2
+0.3
Night
+0.1
+0.2
+0.4
−0.02
−0.01
+0.01
+0.01
+0.025
+0.1
+0.2
+0.3
Core
+0.01
+0.025
+0.1
−0.01
+0.01
+0.025
+0.1
+0.2
+0.3
Mantle
Δ m2
sin 2 2θ V

Figure 5

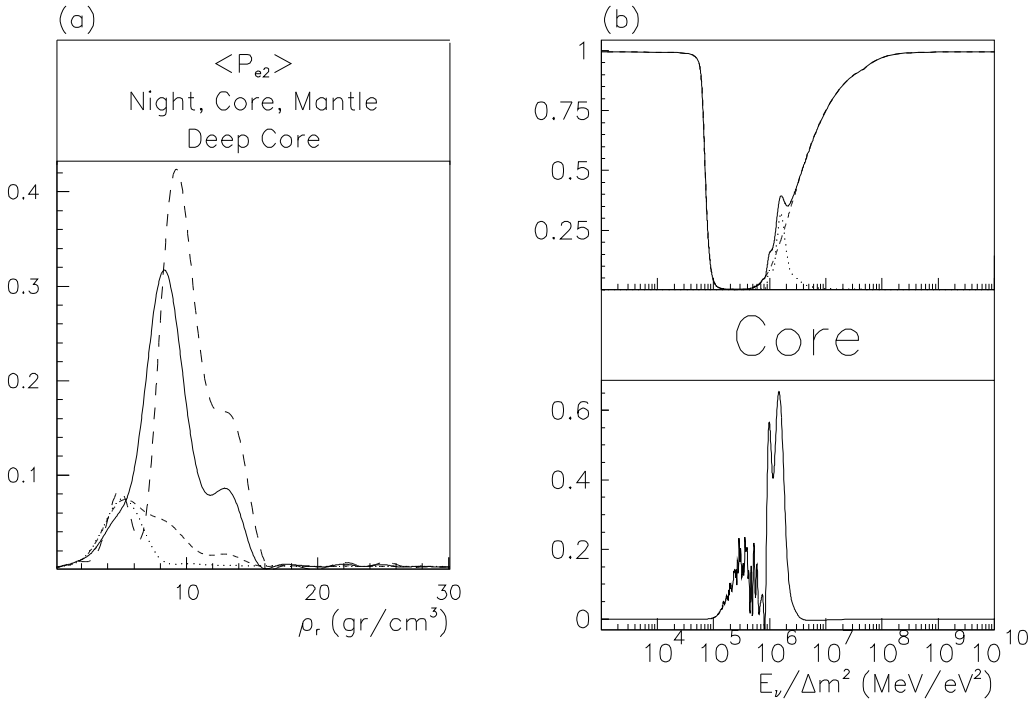


Figure 2. a) $< P_{e2} >$ for *Night* (short dashed line), *Mantle* (dotted line), *Core* (black line) and *Deep - Core* (long dashed line) samples. b): up frame $P_{\oplus}$ (black line), $< P_{e2} >$ (dotted line) and $P_s$ (dashed line) for the *Core* sample; down frame $\mathcal{A}_P(E_\nu/dms)$ for the *Core* sample.

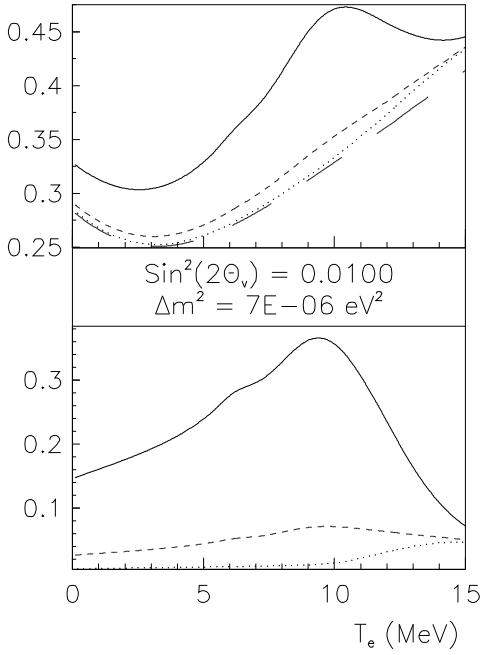


Figure 3. Recoil - $e^-$ spectrum distortion (upper) and D-N asymmetry (lower), for *Day* (long dashed line), *Night* (short dashed line), *Mantle* (dotted line), *Core* (black line) samples.